Supporting Information

Hyaluronic Acid-Modified Au-Ag Alloy Nanoparticles for Radiation/Nanozyme/Ag^+ Multimodal Synergistically Enhanced Cancer Therapy

Yu Chong,[†,‡] Jie Huang,[,‡] Xiaoyu Xu,[‡] Chenggong Yu,[‡] Xingyu Ning,[‡] Saijun Fan,[⊥] Zhijun Zhang[*,‡]*

[†]State Key Laboratory of Radiation Medicine and Protection, School for Radiological and interdisciplinary Sciences (RAD-X) and Collaborative Innovation Center of Radiation Medicine of Jiangsu Higher Education Institutions, Soochow University, Suzhou, 215123, China.

[‡]CAS Key Laboratory of Nano-Bio Interface, Division of Nanobiomedicine, Suzhou Institute of Nano-Tech and Nano-Bionics, Chinese Academy of Sciences, Suzhou, 215123, China.

[⊥] Tianjin Key Laboratory of Radiation Medicine and Molecular Nuclear Medicine, Institute of Radiation Medicine, Chinese Academy of Medical Science/Peking Union Medical College, Tianjin, 300192, China

*Corresponding authors.

Email: jhuang2008@sinano.ac.cn; zjzhang2007@sinano.ac.cn

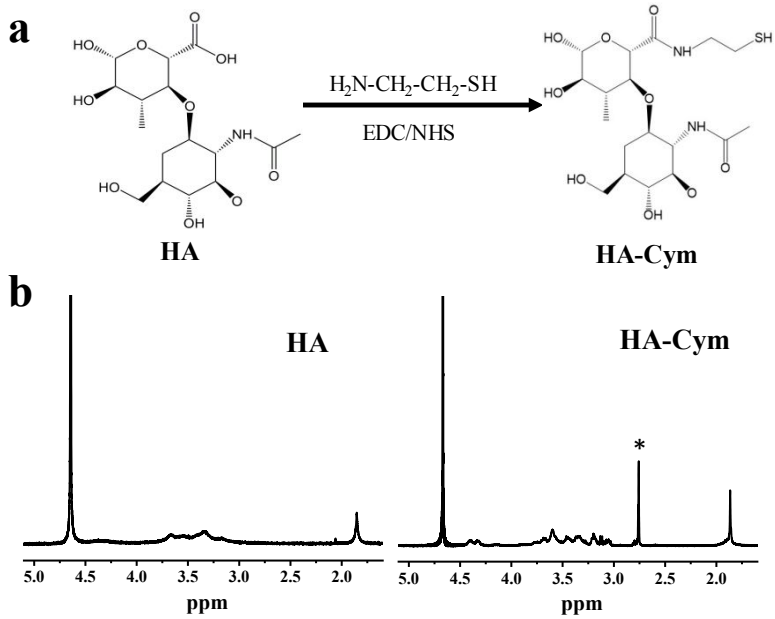

Figure S1. Synthesis and characterization of HA-Cym Conjugates. (a) Formation of HA-Cym conjugates by covalent modification of Cym onto the carboxyl groups of HA *via* amide bonds. (b) ^{1}H NMR spectra of HA and HA-Cym conjugates. Resonance peak at 2.76 ppm marked * was assigned to the methylene protons on –CH_2SH of Cym.

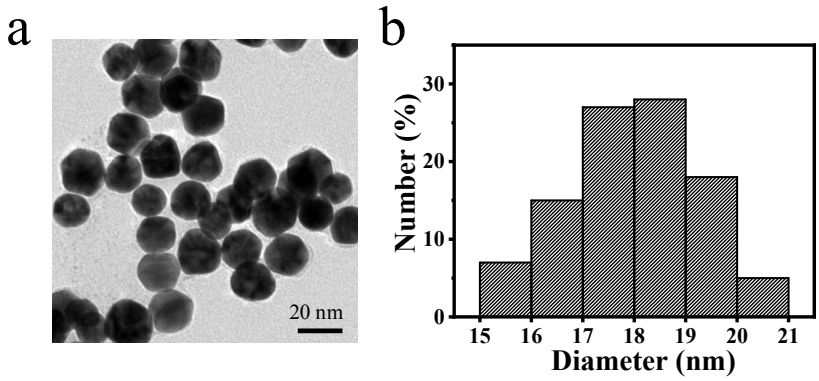

Figure S2. (a) TEM image of Au@HA NPs. (b) Diameter distribution of Au@HA NPs based on the TEM image in (a).

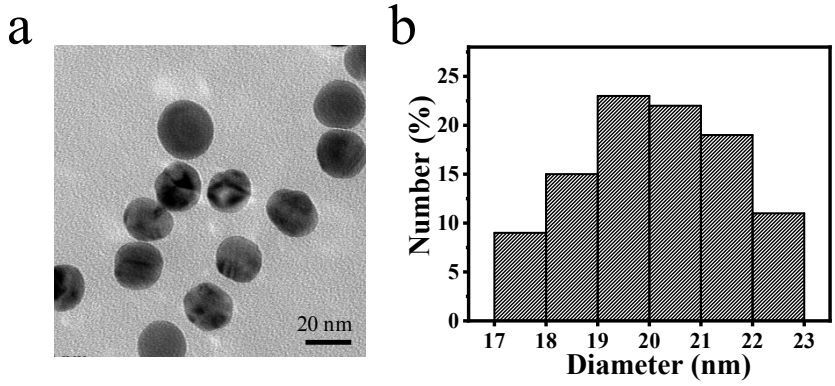

Figure S3. (a) TEM image of Ag@HA NPs. (b) Diameter distribution of Ag@HA NPs based on the TEM image in (a).

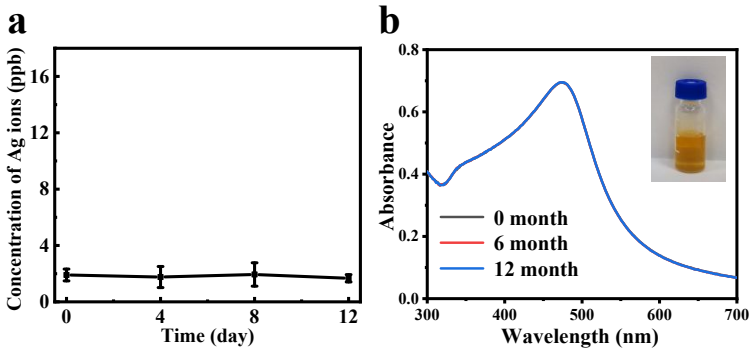

Figure S4. Stability of Au-Ag@HA NPs. (a) Concentration of free Ag^+ in PBS (pH=7.4) of Au-Ag@HA NPs in 12 days determined by ICP-MS, n=3. (b) The UV−vis absorption spectrum for Au-Ag@HA NPs stored at room temperature for 1 year, and a photograph of Au-Ag@HA NPs aqueous solution is shown as inset.

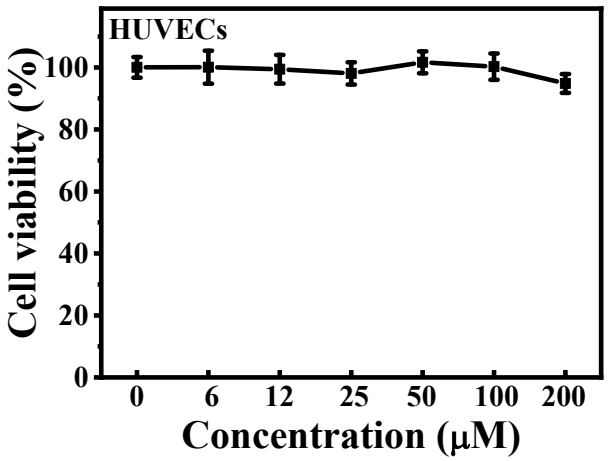

Figure S5. Relative viability of HUVEC cells incubated with Au-Ag@HA NPs at different concentrations for 24 h (n=3).

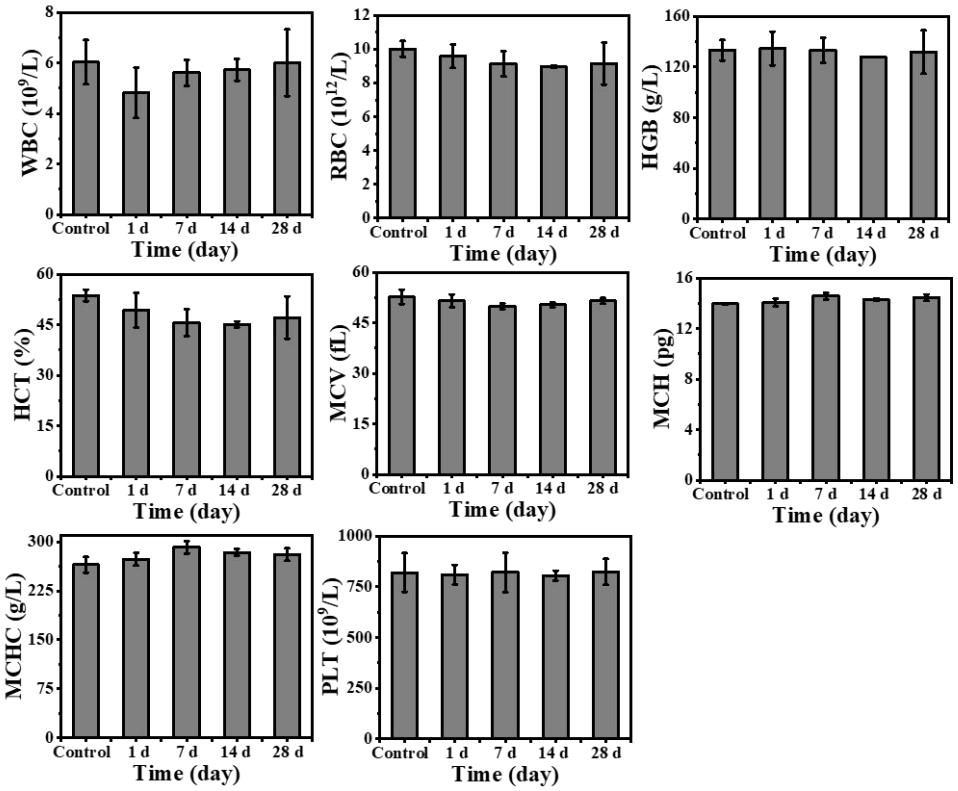

Figure S6. Blood routine analysis for the mice treated with Au-Ag@HA NPs at different time points. Mean values and error bars are defined as mean and standard deviation, n = 5.

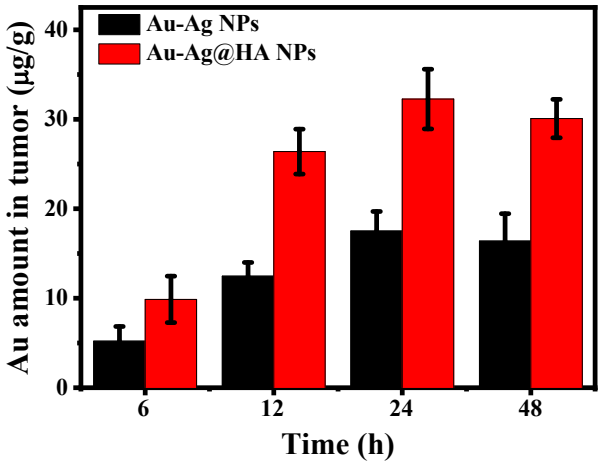

Figure S7. The content of Au element in the tumors from the mice bearing 4T1 tumors after intravenous injection of Au-Ag@HA NPs or Au-Ag NPs for different periods of time. Values represent means ± standard error, n=3.

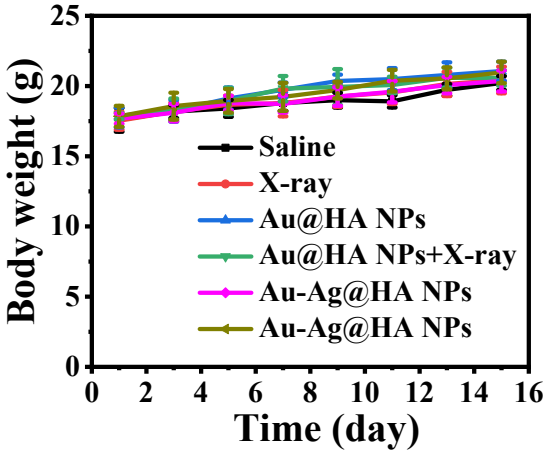

Figure S8. Body weight fluctuation of the mice bearing 4T1 tumors after different treatments: saline alone, saline plus X-ray, Au@HA NPs (10 mg kg^{-1}) alone, Au@HA NPs (10 mg kg^{-1}) plus X-ray, Au-Ag@HA NPs (10 mg kg^{-1}) alone and Au-Ag@HA NPs (10 mg kg^{-1}) plus X-ray.

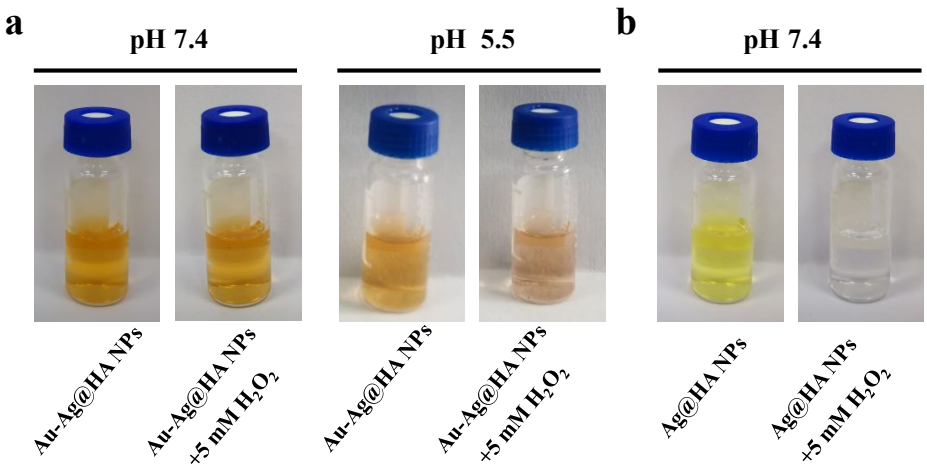

Figure S9. (a) Photographs of Au-Ag@HA NPs with or without 5 mM H_2O_2 at either acidic or neutral solution after 30 min incubation. (b) Photographs of Ag@HA NPs with or without 5 mM H_2O_2 under neutral condition after 30 min incubation.

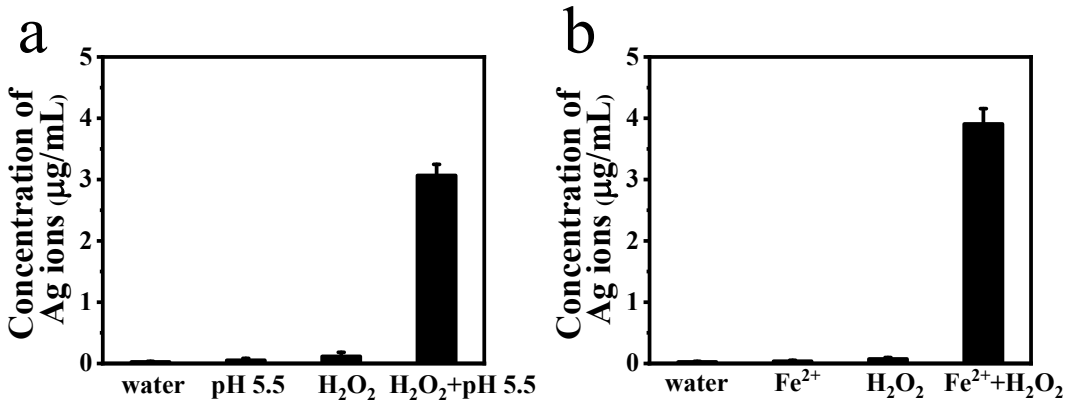

Figure S10. (a) The release of Ag^+ from Au-Ag@HA NPs in the presence of H_2O_2 (5 mM) at pH 5.5 for 30 min. (b) The release of Ag^+ by •OH generated from Fenton reaction ($FeCl_2$ (25 μM) and H_2O_2 (25 μM)) for 10 min.